Lipid-Based Nanocarriers Provide Prolonged Anticancer Activity for Palbociclib: *In Vitro* and *in Vivo* Evaluations

Parichehr Hassanzadeh[1,2], Elham Arbabi[3], Fatemeh Rostami[3]

[1] *Nanotechnology Research Center, School of Pharmacy, Tehran University of Medical Sciences, Tehran, Iran*

[2] *Sasan Hospital, Tehran, Iran*

[3] *Research Center for Gastroenterology and Liver Diseases, Shahid Beheshti University of Medical Sciences, Tehran, Iran*

Received: 28 Nov. 2020; Accepted: 14 Jun. 2021

Abstract- Breast cancer therapy has remained one of the major healthcare challenges. Based on the critical role of cyclin-dependent kinase 4/6 (CDK 4/6) in cell cycle progression, targeting this signaling appears promising for cancer therapy. Palbociclib, a selective CDKs 4/6 inhibitor, is the first-line treatment for estrogen receptor-positive breast cancer. However, poor absorption or side effects may negatively affect its efficiency. This prompted us to incorporate palbociclib into the nanostructured lipid carriers (NLCs) and evaluate the anticancer effect of the nanoformulation (Pa-NLCs) in *in vitro* and *in vivo* models of breast cancer. Pa-NLCs were developed by high-pressure homogenization followed by assessment of the physicochemical characteristics and bioactivities in MCF-7 breast cancer cells and female Wistar rats exposed to the carcinogen 7,12-dimethylbenz(a)anthracene (DMBA). The prepared Pa-NLCs demonstrated suitable physicochemical characteristics, including the controlled release pattern, efficient cellular uptake, and cytotoxicity, while free palbociclib failed to show significant effects. Rats treated with Pa-NLCs exhibited significantly reduced tumor volumes, increased survival rates, and histopathological improvement. Free palbociclib was significantly less efficient than Pa-NLCs. Pa-NLCs, by improving the pharmacological profile of palbociclib and providing longer-lasting effects, can be considered as a promising nanoformulation against breast cancer.

Acta Med Iran 2021;59(6):333-345.

Keywords: Palbociclib; Cyclin-dependent kinase 4/6 (CDK 4/6) inhibitor; Nanostructured lipid carriers; Breast cancer; Michigan cancer foundation-7 (MCF-7) cells; Rat

Introduction

Breast cancer is one of the most common causes of mortality in females (1). Since cell cycle dysregulation and activation of cyclin-dependent kinases (CDKs) are hallmarks of breast cancer, CDKs have been considered attractive targets in cancer treatment (2-5). The limited activity or serious side effects of the first-generation CDK inhibitors led to the development of the next-generation of drugs capable of inhibiting the activity of specific CDK subtypes, including the CDKs 4 and 6 (CDK 4/6), which are critically involved in the initiation and progression of various types of cancers. Following identification of the role of cyclin D1 and CDK4/6 in the pathogenesis of breast cancer (6), the selective CDK 4/6 inhibitors, including abemaciclib, ribociclib, and palbociclib (PD 0332991), were developed against advanced breast cancer (3,7). Palbociclib, a potent and highly selective CDK 4/6 inhibitor, has shown promising growth inhibitory activity against various types of tumors such as hepatocellular, renal cell, and non-small cell lung carcinoma neuroblastoma, multiple myeloma, esophageal adenocarcinoma, and melanoma (8-13). Palbociclib has been most extensively investigated in the field of breast cancer. About 80% of breast tumors express estrogen receptor (ER) and rely on ER signaling for their growth and survival (14). ER inhibition may result in cell cycle arrest in the G_1 phase

Corresponding Author: P. Hassanzadeh
Nanotechnology Research Center, School of Pharmacy, Tehran University of Medical Sciences, Tehran, Iran
Tel: +98 9121887745, Fax: +98 2166581558, E-mail addresses: hassanzadehparichehr4@gmail.com, p-hassanzadeh@razi.tums.ac.ir

and reduction of tumor cell viability (15). In a panel of 47 breast cancer cell lines exposed to palbociclib, ER+cells were the most sensitive ones to growth inhibition (16,17). Regarding the significance of targeting transcription factors for cancer therapy, palbociclib has been shown to inactivate the transcription factor, forkhead box M1 (FOXM1), leading to the anti-proliferation effects (18-20). As monotherapy, palbociclib blocks cell cycle progression via inhibiting hyperphosphorylation of RB protein in breast cancer cells (16). In combination therapy, palbociclib may sensitize cancer cells to ionizing radiation or chemotherapeutic agents (16,17). Palbociclib, in combination with non-steroidal aromatase inhibitor letrozole, has prolonged the progression-free survival in ER+ advanced breast cancer (21,22). The synergistic growth inhibitory activity of palbociclib with trastuzumab, paclitaxel, tamoxifen, or fulvestrant has also been shown (16,22-24). Palbociclib and letrozole have been represented as first-line treatment of ER^+ and epidermal growth factor receptor 2-negative breast cancer (16,22,25,26). Meanwhile, palbociclib may be associated with poor absorption and a variety of side effects (7,16,22,25-31) that may negatively affect the efficiency of the drug. This prompted us to incorporate palbociclib into the nanostructured lipid carriers (NLCs), the colloidal drug carriers with high stability, biocompatibility, and drug loading extent, which are suitable for controlled drug release or targeted delivery and protect the loaded therapeutics against degradation prolong the residence of drugs in target organs and prevent their expulsion during the storage period (32-35). Afterward, we assessed the anticancer activity of nanoformulation in the *in vitro* and *in vivo* models of breast cancer which are relevant to human biology.

Materials and Methods

Materials

Materials for cell culture were obtained from GIBCO/Invitrogen, Germany. Tween 80 and cetyl palmitate were purchased from Merck (Darmstadt, Germany), and other chemicals were purchased from Sigma Aldrich, Germany.

Preparation of palbociclib-loaded NLCs (Pa-NLCs)

The lipid phase containing the oleic acid and cetyl palmitate (15:85 or 30:70) was prepared at 75° C followed by the addition of palbociclib (5, 10, 20, 40, and 100 % w/w). The aqueous phase was provided at the same temperature and added to the lipid phase. Drug-loaded or blank NLCs were developed as previously described in detail (32-35).

Characterization of Pa-NLCs

Determination of the particle size, zeta potential (ZP), and polydispersity index (PDI)

Following re-dispersion, particle size, ZP, and PDI of NLCs were evaluated by photon correlation spectroscopy (Zetasizer Nano, Malvern Instruments, UK), (n=6).

Morphological evaluation of NLCS

Using a scanning electron microscope (KYKY-EM3200, KYKY Technology Development Ltd., China), the shape of lyophilized NLCs was evaluated.

Assessment of drug loading (DL) and entrapment efficiency (EE)

0.5 ml of Pa-NLCs dispersion was centrifuged at 10000 rpm for 40 min, and the amount of palbociclib in the supernatant was determined by HPLC [Hitachi Model D-7000, Merck-Hitachi, Darmstadt, Germany, equipped with a UV-Vis detector (Merck-Hitachi, L-4250, Germany) with C18 column]. The mobile phase included 0.1% triethylamine and acetonitrile (30:70, v/v), and peak absorption wavelength was recorded at 263 nm. Dilutions of palbociclib (10-300 μg/ml) were provided to construct the calibration curve. The limits of detection and quantification were 1.59 and 4.18 μg/ml, respectively. DL% and EE% were determined as follows:

$$EE\% = \frac{\text{Total amount of palbociclib} - \text{the amount of free palbociclib}}{\text{The total amount of palbociclib}} \times 100$$

$$DL\% = \frac{\text{The amount of palbociclib encapsulated in NLCs}}{\text{The total amount of NLCs}} \times 100$$

Differential scanning calorimetry (DSC)

DSC apparatus (Mettler-Toledo, Switzerland) was applied for thermal analysis of cetyl palmitate, palbociclib, lyophilized Pa-NLCs, and blank NLCs. An aluminum pan was used for sample placement followed by heating at the range of 10-280° C (10° C/min).

Assessment of the *in vitro* release profile

The release pattern of palbociclib from NLCs was assessed using dialysis membrane technique (32-34,36).

Dose released percentage was plotted against time and palbaociclib solution was considered as control. Experiments were performed in triplicate.

Stability of nanoparticles during storage at 4° C

Lyophilized samples were re-suspended at 0, 1, 3, and 6 months followed by evaluating the particle size, ZP, PDI, DL%, and EE%. The results were demonstrated as mean±SEM (n=6).

Assessment of the bioactivity of Pa-NLCs *in vitro*

Cell culture

MCF-7 breast cancer cells were cultured in RPMI-1640 medium supplemented with fetal bovine serum (10%), amphotericin B (0.25 µg/ml), penicillin G sodium (100 U/ml), and streptomycin sulfate (100 µg/ml) in 5% CO_2 incubator (Tuttlingen, Germany) at 37° C.

Evaluating the cellular uptake of NLCs

Following loading red fluorescent probe (DiI) into the NLCs, Amicon® filter (Millipore, USA) with molecular weight cut-off of 100 kDa was used for removing the un-encapsulated DiI by centrifugation at 13000 g for 30 min. Fluorescence detector (W2475) was applied for quantification of DiI and chromatography was carried out on C18 column at flow rate of 1 ml/min using the mobile phase including the methanol and 0.05 M dimethyl sulfate (98:2 v/v). Emission and excitation wavelengths were 565 and 549 nm, respectively. Standard curve was linear in the range of 0.005-10 µg/ml with R^2 of 0.99. Limits of detection and quantification were 0.001 and 0.0028 µg/ml, respectively. For evaluation of the cellular uptake of NLCs by confocal microscopy (Nikon, Japan), cells in 6-well plates (2×10^5 cells/well) were incubated with NLCs for 1, 4, and 6 h. For quantitative assessment of the cellular uptake, mean fluorescence intensity was determined by flow cytometer (FACSCalibur, USA) using CellQuest Pro software. Experiments were carried out in triplicate and untreated cells served as control.

Assessment of the cytotoxicity

24 and 48 after treatment with palbociclib (100, 150, 200, and 300 nM), Pa-NLCs (containing 100, 150, 200, and 300 nM palbociclib), or blank NLCs, the viability of MCF-7 cells was assessed by MTT (32-34). Cell viability was expressed as mean±SEM (n=6).

Morphological analysis of MCF-7 cells following exposure to palbociclib or Pa-NLCs

Cells in 6-well plates (10^5 cells/well) were treated with 100, 150, 200, or 300 nM palbociclib or Pa-NLCs (containing 100, 150, 200, or 300 nM palbociclib) for six days followed by fixation in 4% paraformaldehyde for 30 min, washing with PBS (0.02 M), and staining with Hoechst 33258 (32,34). Images were captured by fluorescence microscope (Leica, Germany). In each group, the morphologically altered cells were counted in six visual fields and the percentage over total number of cells was determined as previously described (37).

***In vivo* experiments**

Animals

Female Wistar rats weighing 140-160 g from the experimental animal center of Pasteur institute (Tehran, Iran) were randomly assigned and housed 3 per cage under the standard laboratory conditions; temperature (24±2° C), humidity (55±10%), with a 12-h light/dark cycle and *ad libitum* access to water and food pellets. Animal experiments were carried out in accordance with the European Committee guidelines for the use of experimental animal and were approved by the local ethics committee.

Inducing breast cancer and treatment groups

Breast cancer was induced by subcutaneous injection of 7,12-dimethylbenz (a) anthracene (DMBA) at dose of 100 mg/kg (38,39), (group 1). Other groups received intravenous injections three times a week as follows; groups 2-5 received 10, 30, or 75 mg/kg of palbociclib (dissolved in sodium lactate (50 mM, pH 4) (40-43) or vehicle, groups 6-9 received Pa-NLCs (containing 10, 30, or 75 mg/kg of palbociclib) or blank NLCs. Injections were initiated two weeks before DMBA administration and continued for 12 weeks. Animals were checked twice a week for body weight alterations, abnormal mass, and mortality. According to the relevant animal studies, n=6/group was selected for statistical analysis.

Determining the tumor volume

Tumor volumes were determined by a caliper and following formula:

$V\ (mm^3) = (ab^2\pi)/6$

(*a*: the largest diameter of tumor, *b*: the largest diameter of tumor at 90 degrees to *a*).

Histological evaluation

Animals were anesthetized by intramuscular injection of 80 mg/kg of ketamine-HCl and 10 mg/kg of xylazine followed by mammary gland isolation,

cleaning, drying, weighing, immersion of mammary glands in Bouin's solution overnight, dehydration, paraffin embedment, providing 5-μm thick sections by rotary microtome (Leica, Germany), mounting on the glass slides, and hematoxylin-eosin staining (38,44,45). Samples were visualized using the microscope (Wolfe, S9-0982, Germany) and photos were captured by digital camera (Canon, Power-Shot SX500).

Data analysis

Shapiro-Wilk test was used to verify normal data distribution. Analysis of variance (ANOVA) followed by Tukey's test was used for analysis of data related to the physicochemical properties of NLCs and their stability, drug release profile *in vitro*, cytotoxicity, alterations of body weights, and tumor volumes. Mann-Whitney *U* test was used for evaluating the morphological alterations of cells. Statistical significance in the survival evaluation (plotted as Kaplan-Meier curves) was evaluated by Log-rank test. Data have been demonstrated as mean±SEM with significance level of $P<0.05$.

Results

Characterizing of Pa-NLCs

Using various ratios of liquid and solid lipids, palbociclib and lipid, and sonication time or surfactants, several formulations of Pa-NLCs were developed (Table 1). Using higher amounts of surfactant and oil lipid led to higher EE% and smaller size of particles. Considering DL% and EE%, Pa-NLCs-8 was determined as the optimum formulation (Table 1). As shown in Figure 1, spherical shapes of Pa-NLCs were preserved even three months after lyophilization. In DSC, palbociclib showed an endothermic peak at 269.43° C (Figure 2b) and the melting peak of Pa-NLCs was observed at 74.83° C (Figure 2a). Cetyl palmitate showed a melting peak at 54.73° C (Figure 2c) and blank NLCs demonstrated a melting peak at 52.17° C (Figure 2d). Palbociclib release from solution was faster than Pa-NLCs formulation which demonstrated controlled drug release profile (Figure 3).

The stability of lyophilized nanoparticles were preserved without remarkable changes of the physicochemical properties (Table 2, $P>0.05$).

Table 1. Physicochemical characteristics of various Pa-NLCs formulations

Formulation code	Particle size (nm)	PDI	ZP (mV)	EE (%)	DL (%)	DR after 48 h (%)
Pa-NLCs-1	134.6 ± 7.9	0.33 ± 0.07	-23.7 ± 0.39	43.5 ± 2.7	1.43 ± 0.14	52.7 ± 4.5
Pa-NLCs-2	121.8 ± 7.2	0.37 ± 0.05	-24.6 ± 0.37	47.8 ± 4.2	1.38 ± 0.05	53.4 ± 3.9
Pa-NLCs-3	109.3 ± 8.5	0.25 ± 0.03	-23.9 ± 0.43	63.4 ± 3.8	1.57 ± 0.13	62.9 ± 3.7
Pa-NLCs-4	65.3 ± 3.2	0.17 ± 0.05	-25.3 ± 0.36	90.3 ± 5.7	3.56± 0.07	82.3 ± 3.3
Pa-NLCs-5	76.5 ± 3.9	0.19 ± 0.05	-22.5 ± 0.47	94.6 ± 6.2	5.93 ± 0.15	77.8 ± 5.2
Pa-NLCs-6	89.7 ± 3.4	0.26 ± 0.07	-19.2 ± 0.33	85.3 ± 4.5	11.86 ± 2.3	74.3 ± 3.5
Pa-NLCs-7	93.9 ± 2.7	0.29 ± 0.03	-28.9 ± 0.55	94.3 ± 7.3	28.32 ±2.5	65.7± 2.7
Pa-NLCs-8	132.8 ± 5.4	0.23 ± 0.05	-25.7± 0.45	87.9 ± 5.5	45.92 ± 3.7	63.9 ± 3.8
Blank NLCs	52.9 ± 4.6	0.17 ± 0.03	-18.8 ± 0.37	_	_	_

Data are expressed as mean±SEM (n=6)
(ZP: zeta potential, PDI: polydispersity index, DL: drug loading, EE: entrapment efficiency, DR: drug release, Pa-NLCs: palbociclib-loaded nanostructured lipid carriers)

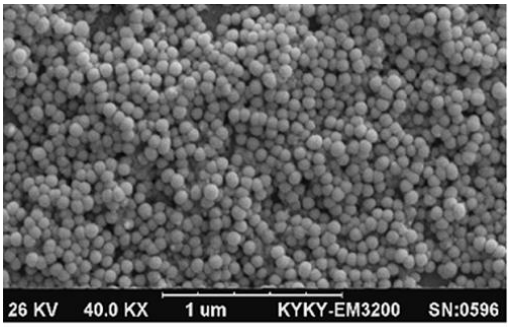

Figure 1. Scanning electron micrographs of Pa-NLCs. Well-dispersed nanoparticles have preserved their spherical shapes even three months after lyophilization
(Pa-NLCs: Palbociclib-loaded nanostructured lipid carriers)

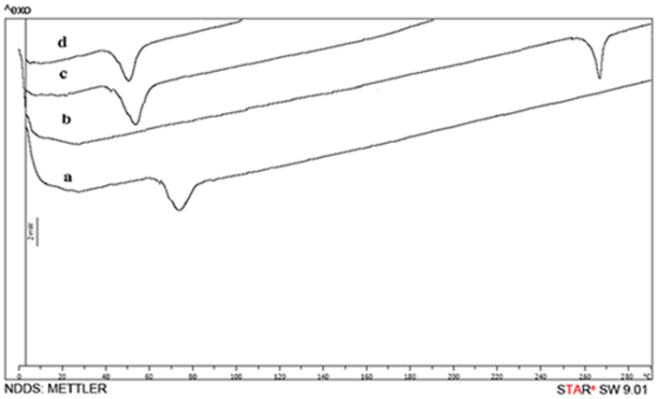

Figure 2. DSC thermograms. a: Pa-NLCs, b: palbociclib, c: cetyl palmitate, d: blank NLCs

(DSC: differential scanning calorimetry, Pa-NLCs: Palbociclib-loaded nanostructured lipid carriers)

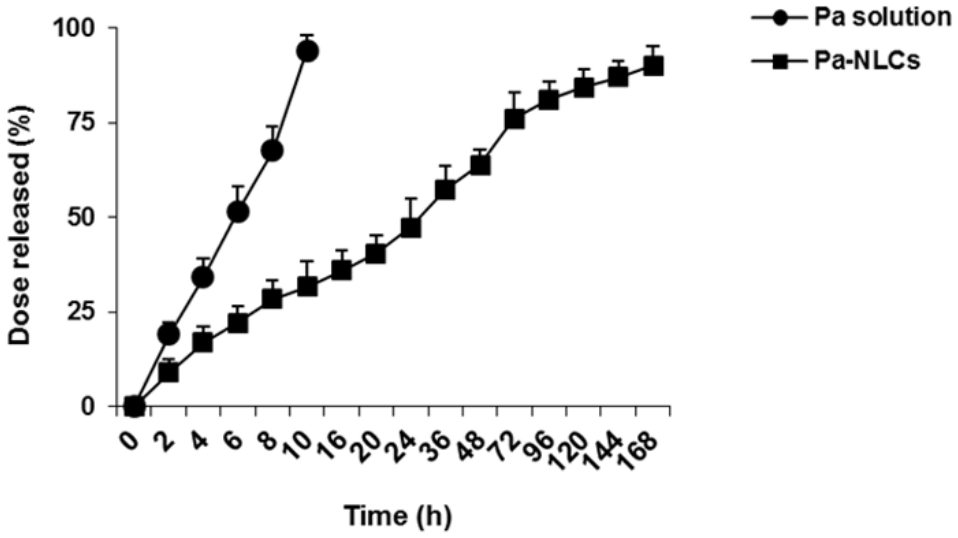

Figure 3. The release pattern of palbociclib *in vitro*. Palbociclib demonstrated a controlled release profile from Pa-NLCs. Data are demonstrated as mean±SEM (n=3). (Pa-NLCs: Palbociclib-loaded nanostructured lipid carriers)

Table 2. Stability profile of Pa-NLCs

Initial					**1st Month**				
Size	PDI	ZP	EE%	DL%	Size	PDI	ZP	EE%	DL%
132.8±5.4	0.23±0.05	-25.7± 0.4	87.9±5.5	45.9±3.7	135.5±4.9	0.22±0.03	-25.4±0.7	85.5±4.7	42.7±2.5
3rd Month					**6th Month**				
Size	PDI	ZP	EE%	DL%	Size	PDI	ZP	EE%	DL%
139.5±3.5	0.25±0.07	-26.5±0.9	80.7±5.3	39.8±0.4	141.7±3.9	0.28±0.09	-25.6±0.3	77.36±2.9	37.3±1.5

Data are demonstrated as mean ± SEM (n=6).
(Pa-NLCs: palbociclib-loaded nanostructured lipid carriers, ZP: zeta potential, PDI: polydispersity index, DL: drug loading, EE: entrapment efficiency)

Evaluation of the cellular uptake

Using the confocal microscopy, cellular uptake of DiI-loaded NLCs was visualized (Figure 4A-4C). 4 and 6 h after exposure, remarkable enhancement of fluorescence intensity was observed (Figure 4D, $P<0.05$ and $P<0.01$).

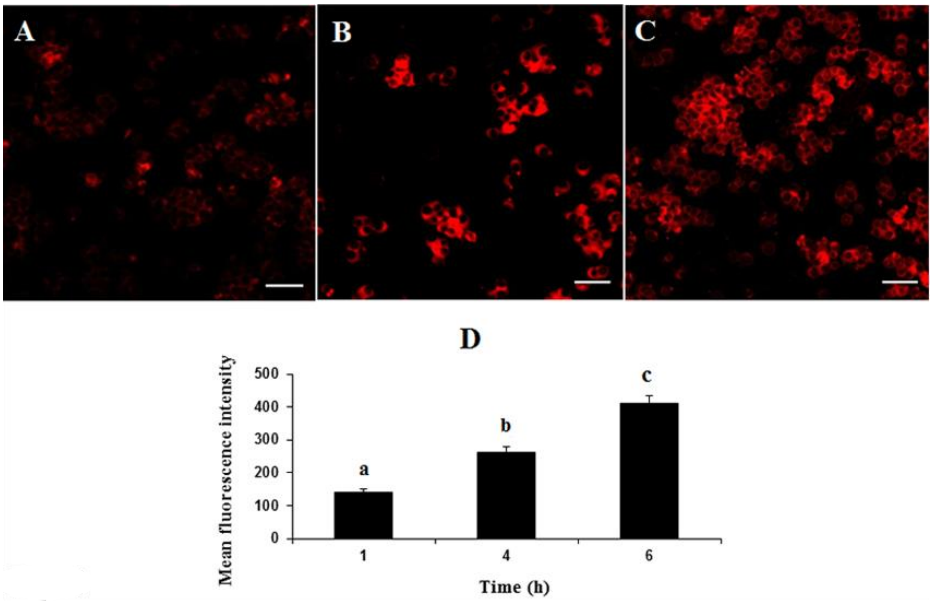

Figure 4. Cellular uptake of DiI-loaded NLCs. A-C: Confocal microscopy images regarding the cellular uptake of DiI-loaded NLCs after 1, 4, and 6 h of incubation, respectively (sale bars = 20 µm), D: mean fluorescence intensity values following 1, 4, and 6 h (a-c, respectively) of incubation with NLCs. Data are expressed as mean±SE (n = 3). [b] $P<0.05$ *vs*. a and c, [c] $P<0.05$ *vs*. b and $P<0.01$ *vs*. a.

Assessment of the cell viability

24 and 48 h after treatment with Pa-NLCs (containing 200 or 300 nM palbociclib), cell viability was significantly reduced (Figure 5A and 5B, $P<0.05$, $P<0.01$, and $P<0.001$ *vs*. control), while free palbociclib did not significantly affect cell viability at any dose tested (Figure 5A and 5B, $P>0.05$ *vs*. control).

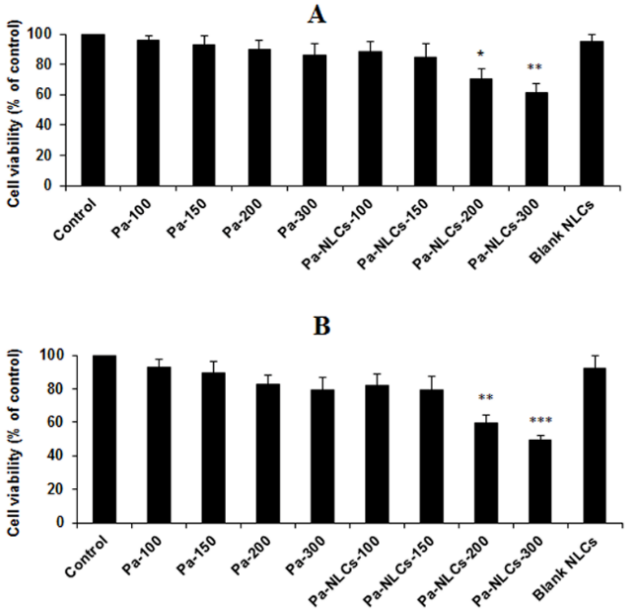

Figure 5. Assessment of cell viability in MCF-7 cell culture exposed to palbociclib or Pa-NLCs. 24 and 48 after treatment (A and B, respectively), the viability of MCF-7 cells was evaluated by MTT assay. Pa-NLCs dose-dependently reduced the cell viability, while free palbociclib failed to exert a significant effect at equivalent doses. Data are presented as mean ± SEM of 6 experiments. (Pa-100, 150, 200, and 300: treatment with palbociclib (100, 150, 200, and 300 nM), Pa-NLCs-100, 150, 200, and 300: treatment with Pa-NLCs (containing 100, 150, 200, and 300 nM palbociclib). Pa-NLCs: palbociclib-loaded nanostructured lipid carriers. $^{*}P<0.05$, $^{**}P<0.01$, and $^{***}P<0.001$ *vs.* control

Morphological evaluation of MCF-7 cells

As compared to the control (Figure 6A), six-day treatment with 200 or 300 nM palbociclib did not significantly affect cellular morphology (Figure 6B and 6C, respectively), while altered cellular morphology (condensed nuclei) was observed following six-day exposure to Pa-NLCs (containing 200 or 300 nM palbociclib, Figure 6D, and 6E, respectively). Damaged cells were significantly increased in Pa-NLCs groups (Figure 6F, $P<0.01$ and $P<0.001$ *vs.* palbociclib-treated groups and $P<0.001$ *vs.* control). In palbociclib-treated groups, the number of the morphologically altered cells did not significantly differ from that in the control group (Figure 6F, $P>0.05$).

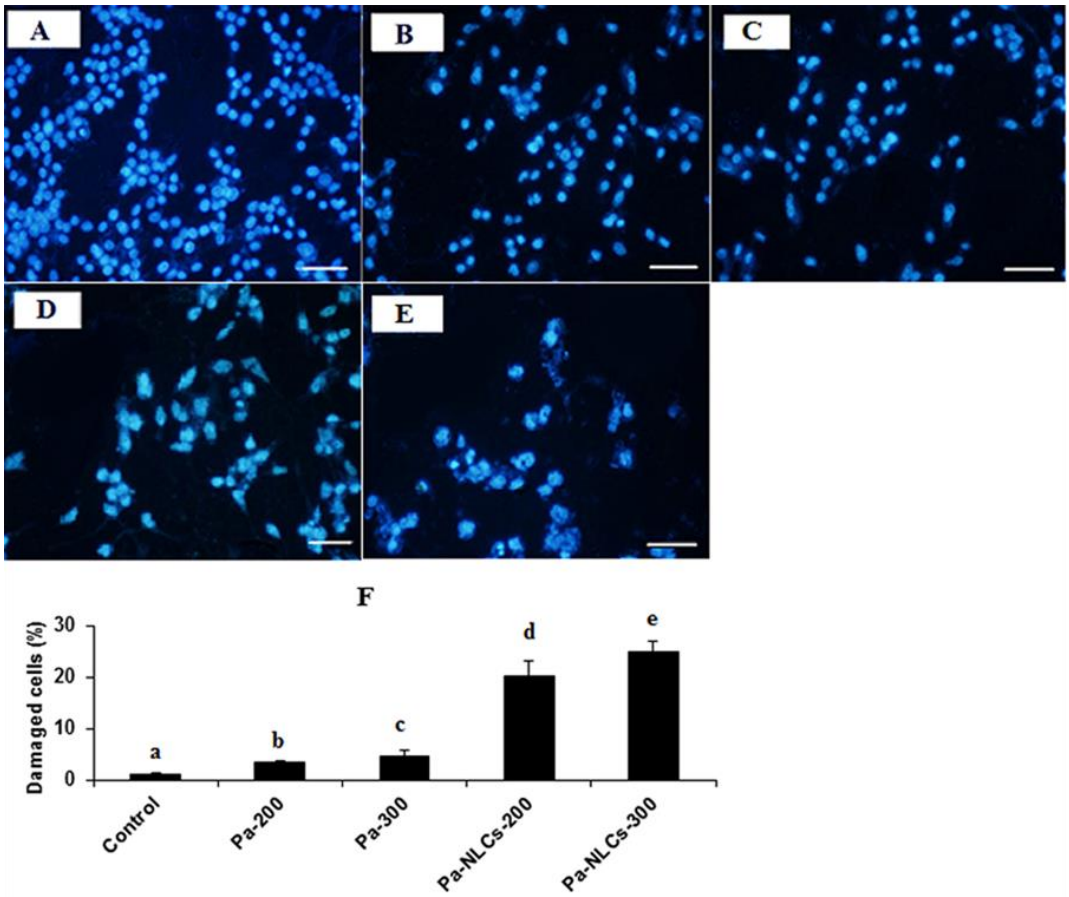

Figure 6. Morphological evaluation of MCF-7 cells. Hoechst stain was used for assessment of the cellular damage after six-day exposure to free palbociclib or Pa-NLCs

A: control cells, B and C: treatment with palbociclib (200 and 300 nM, respectively) did not significantly affect cellular morphology, D and E: alterations of the cellular morphology (increased condensed nuclei) after treatment with Pa-NLCs (containing 200 and 300 nM palbociclib, respectively). (Scale bars = 20 μm), F: Morphologically-altered cells presented as the percentage of total cells counted. Data are expressed as mean±SEM (n=6). [d] $P< 0.01$ *vs.* c and $P< 0.001$ vs. a and b, [e] $P< 0.001$ vs. a, b, and c. (Pa-NLCs: palbociclib-loaded nanostructured lipid carriers)

***In vivo* studies**

Effects of DMBA, palbociclib, and Pa-NLCs on the bodyweight

A significant reduction of body weight was observed in DMBA-treated rats (Table 3, $P<0.01$ *vs.* the vehicle- and blank NLCs-treated groups). Furthermore, palbociclib and (75 mg/kg) and Pa-NLCs (containing 75 mg/kg of palbociclib) significantly reduced body weight ($P<0.05$ *vs.* vehicle- and blank NLCs-treated groups), however, a significant difference was observed between palbociclib- and Pa-NLCs-treated groups ($P<0.05$).

Table 3. Effects of DMBA, palbociclib, and Pa-NLCs on the bodyweight

Experimental groups	Initial body weight (g)	Final body weight (g)
Vehicle	146.3 ± 6.2	398.9 ± 10.7
Blank NLCs	148.7 ± 5.4	383.7 ± 12.3
DMBA	151.5 ± 5.9	193.5 ± 7.5 [a]
Palbociclib+DMBA	154.8 ± 3.7	204.3 ± 3.2 [b]
Pa-NLCs+DMBA	146. 3 ± 9.3	297.7 ± 5.9 [c]
Blank NLCs+DMBA	153.6 ± 6.7	199.6 ± 9.7 [a]

Data are expressed as mean ± SEM (n=6). [a] $P< 0.01$ *vs.* the vehicle- and blank NLCs-treated groups, [b] $P<0.05$ *vs.* vehicle- and blank NLCs-treated groups, [c] $P<0.05$ *vs.* vehicle-, blank NLCs, and palbociclib+DMBA-treated groups. (Pa-NLCs: palbociclib-loaded nanostructured lipid carriers), c *vs.* b: $P<0.05$.

Effects of palbociclib and Pa-NLCs on the survival rate following treatment with DMBA

Treatment with Pa-NLCs formulation (containing 75 mg/kg of palbociclib) provided a significantly higher survival rate ($P<0.01$) as compared to free palbociclib (75 mg/kg), blank NLCs-, or DMBA-treated group (Figure 7).

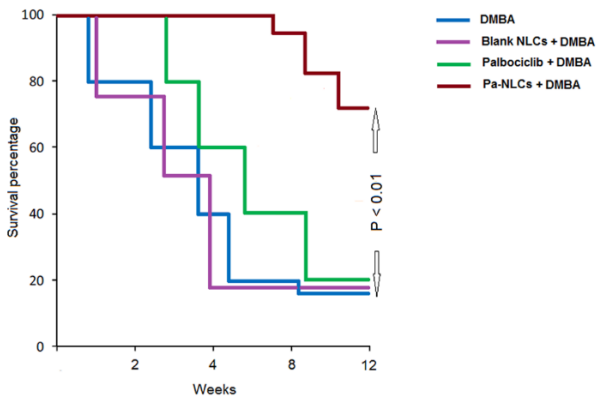

Figure 7. Kaplan-Meier curves demonstrating the survival data in DMBA-treated rats exposed to palbociclib, Pa-NLCs, or blank NLCs. The difference between the survival curves was evaluated by a log-rank test. (Pa-NLCs: palbociclib-loaded nanostructured carriers)

Effects of DMBA, palbociclib, and Pa-NLCs on tumor growth

DMBA induced significant tumor growth ($P<0.05$, $P<0.01$, and $P<0.001$ *vs.* the group treated with Pa-NLCs). Palbociclib even at the highest dose tested (75 mg/kg) did not significantly affect tumor growth as compared to the vehicle-, blank NLCs, and DMBA-treated groups (Figure 8, $P>0.05$), while, Pa-NLCs (containing 75 mg/kg of palbociclib) significantly reduced tumor volume (Figure 8, $P<0.05$, $P<0.01$, and $P<0.001$ *vs.* other groups as mentioned in the figure legend).

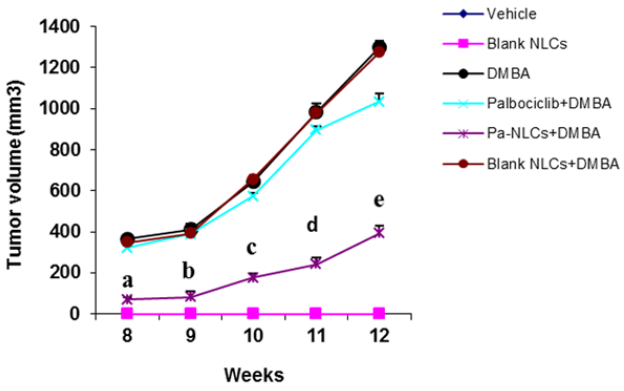

Figure 8. Effects of palbociclib and Pa-NLCs on tumor volume in DMBA-treated animals. a and b: $P<0.05$ *vs.* all groups receiving DMBA, c: $P<0.05$ *vs.* the vehicle and blank NLCs groups and $P<0.01$ *vs.* the DMBA-treated groups, d: $P<0.01$ *vs.* the vehicle and blank NLCs groups and $P<0.001$ *vs.* the groups receiving DMBA, e: $P<0.001$ *vs.* the vehicle and blank NLCs groups and DMBA-treated groups

Effects of palbociclib and Pa-NLCs on DMBA-induced histopathological alterations

DMBA-induced histopathological alterations, including the dilated ducts and hyper-chromatic nuclei and eosinophilic cytoplasms in the luminal cells (Figure 9B), were improved following treatment with Pa-NLCs

(containing 75 mg/kg palbociclib) (Figure 9D). Reduced amounts of connective tissues and dilated ducts were observed in animals treated with free palbociclib (75 mg/kg) (Figure 9C).

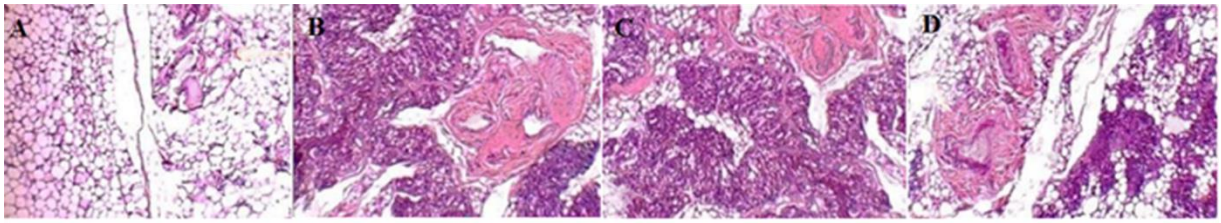

Figure 9. Effects of palbociclib and Pa-NLCs on DMBA-induced histopathological alterations. A: mammary glands in the control animals demonstrated normal histological patterns, B: morphological alterations including the hyper-chromatic nuclei and eosinophilic cytoplasms in the luminal cells and dilated ducts in carcinogen-treated animals, C: reduced amounts of connective tissues and dilated ducts in animals treated with free palbociclib (75 mg/kg), D: moderate lymphocytic infiltration following treatment with Pa-NLCs (containing 75 mg/kg palbociclib), (magnifications; A-C: 400 x, D: 10 x)

Discussion

Treatment of breast cancer has remained one of the major healthcare challenges. In recent years, targeting the cell cycle and inhibition of CDKs have gained considerable attention. Selective CDK4/6 inhibitors have shown therapeutic potentials against various types of tumors. Palbociclib, which is a highly selective inhibitor of CDKs 4/6, has been approved as the first-line treatment of ER^+ breast cancer. However, poor solubility and frequency- or dose-related side effects (7,16,22,25,26) may negatively affect its efficiency. Over the last decades, increasing research efforts in nanotechnology have resulted in the development of biocompatible nanostructures and optimized nanocarriers in order to protect the encapsulated drugs or biomolecules against excretion or metabolism and overcome the potential chemo-resistance. High-resolution imaging, real-time detection of a variety of biomarkers, controlled drug delivery, and targeted therapy may improve the efficiency of therapeutics and reduce their side effects. In this context, several nanoformulations with improved bioavailability and half-lives have proved to be useful against a variety of disorders (46-49). The development of nanotechnology-based imaging techniques facilitates detection of early-stage tumors or identification of the molecular expressions of neoplasms (50). Application of the nanobiosensors or nanowires for early detection of malignant lesions (51,52) might be of critical significance in cancer treatment. Using paramagnetic nanoparticles or polymeric dendrimers for detection of lymph node metastases (53,54), bimodal nanoparticles for intra-operative visualization of lesions (55), nanoparticle probes targeted with recognition agents for detecting tumor markers (56), or metal-based nanovectors for thermal ablation of tumors (57) indicate the significance of nanotechnology-based approaches in designing the novel generations of anticancer therapeutics.

In order to overcome the problems associated with older nanomaterials, advanced nanocarriers, including lipid-based colloidal drug delivery systems, have been designed. This type of nanoparticle facilitates targeted drug delivery, protects the encapsulated therapeutic agents against degradation, and improves their bioavailability and efficiency. Because of the limitations of solid lipid nanoparticles, such as the limited capacity of drug loading or drug expulsion, NLCs are preferred for the incorporation of poorly water-soluble drugs (35). Application of NLCs with suitable biocompatibility, long-term stability, high capacity of drug loading, and controlled drug release pattern may lead to improved pharmacological profiles, reduced dose frequency, and side effects of drugs (32-35,58). Besides its usefulness against fungal infections or ischemic neural injuries, the application of NLCs may improve the therapeutic index of encapsulated anticancer drugs (59,60). Loading of tyrphostin AG-1478, an inhibitor of epidermal growth factor receptor, into NLCs has provided promising therapeutic effects in human hepatocarcinoma cells (61). Based on this background, we have encapsulated palbociclib into the NLCs for obtaining longer-lasting therapeutic effects. During six months of storage, Pa-NLCs demonstrated high stability profile (Table 2) that may be related to the binary lipid mixture, increased imperfection, and reduced expulsion of palbociclib. The spherical shapes of Pa-NLCs with the suitable distribution of particle size and ZP were maintained during the storage period (Table 1, Figure 1) that may be

due to the application of appropriate materials and preparation methods.

Using DSC, thermal behaviors of Pa-NLCs, bulk materials, and blank NLCs were evaluated (Figure 2). The disappearance of the endothermic peak of palbociclib in the DSC thermogram of Pa-NLCs indicates drug distribution in the amorphous state. Shifting of the melting curve peaks of Pa-NLCs and blank NLCs to the lower temperatures suggests the transformation of bulk materials into the nanoparticulate formation, increased surface area of particles, lower-ordered positioning of NLCs, and small size of particles. The melting point of Pa-NLCs was lower than that of blank NLCs (Figure 2), which may be due to the encapsulation of palbociclib into the lipid matrix and defect elevation in the crystal lattice.

Palbociclib showed a controlled-release profile from the NLCs (Figure 3) that might be due to the interactions between the lipid-surfactant or lipid-palbociclib, drug partitioning between the aqueous and lipid phases, or drug diffusion from the lipid core. This type of release profile which provides a sustained drug concentration for longer periods of time, might be of key therapeutic importance.

Following the efficient cellular uptake of NLCs (Figure 4), the MTT assay demonstrated that Pa-NLCs, but not free palbociclib, exhibit cytotoxic effects in a dose-dependent fashion (Figure 5). Unlike free palbociclib, six-day exposure to Pa-NLCs induced cellular damage in a dose-dependent manner (Figure 6). These findings represent NLCs as promising nano reservoirs capable of providing sustained drug concentrations that may result in the increased therapeutic efficiency.

Alterations of body weights were routinely monitored as a sign of *in vivo* toxicity. A significant loss of body weight was observed in animals treated with DMBA, free palbociclib, or Pa-NLCs (Table 3). Meanwhile, weight loss in Pa-NLCs-treated rats was statistically lower than those receiving free palbociclib (Table 3), indicating the reduced toxicity of the drug due to the application of NLCs.

As shown in Figure 8, Pa-NLCs significantly inhibited tumor growth. This might be of therapeutic significance because of the key role of cell proliferation in the process of carcinogenesis, including the initiation and progression (62,63). Higher survival rate and improved DMBA-induced histopathological alterations by Pa-NLCs (Figures 7 and 9) demonstrated higher efficiency of nanoformulation as compared to the free drug.

Nanotechnology, by which a variety of biomaterials or advanced devices may be designed for targeted therapy or early diagnosis of disorders, has opened up new frontiers in biomedical research. Using nanotechnology-based tools provides possibilities to acquire a better understanding of the pathophysiology of various diseases and develop efficient drug delivery systems that might improve treatment outcomes. The development of nanoformulations with increased bioavailability and reduced toxicity which interact with the biological systems may be of key therapeutic importance. In the present study, NLCs have been shown as promising nano reservoirs for encapsulation and delivery of palbociclib with therapeutic potentials against a variety of malignancies. Pa-NLCs via improvement of the pharmacological profile of palbociclib appears as a suitable nanoformulation that provides prolonged effects leading to the reduced dose frequency and side effects of palbociclib.

References

1. Siegel RL, Miller KD, Jemal A. Cancer Statistics, 2017. CA Cancer J Clin 2017;67:7-30.
2. Lange CA, Yee D. Killing the second messenger: targeting loss of cell cycle control in endocrine-resistant breast cancer. Endocr Relat Cancer 2011;18:C19-24.
3. Finn RS, Aleshin A, Slamon DJ. Targeting the cyclin-dependent kinases (CDK) 4/6 in estrogen receptor-positive breast cancers. Breast Cancer Res 2016;18:17.
4. Otto T, Sicinski P. Cell cycle proteins as promising targets in cancer therapy. Nat Rev Cancer 2017;17:93-115.
5. Spring L, Bardia A, Modi S. Targeting the cyclin D-cyclin-dependent kinase (CDK) 4/6-retinoblastoma pathway with selective CDK 4/6 inhibitors in hormone receptor-positive breast cancer: rationale, current status, and future directions. Discov Med 2016;21:65-74.
6. Dickson C, Fantl V, Gillett C, Brookes S, Bartek J, Smith R, et al. Amplification of chromosome band 11q13 and a role for cyclin D1 in human breast cancer. Cancer Lett 1995;90:43-50.
7. Asghar U, Witkiewicz AK, Turner NC, Knudsen ES. The history and future of targeting cyclin-dependent kinases in cancer therapy. Nat Rev Drug Discov 2015;14:130-46.
8. Altenburg JD, Farag SS. The potential role of PD0332991 (Palbociclib) in the treatment of multiple myeloma. Expert Opin Investig Drugs 2015;24:261-71.
9. Rivadeneira DB, Mayhew CN, Thangavel C, Sotillo E, Reed CA, Grana X, et al. Proliferative suppression by CDK4/6 inhibition: complex function of the

retinoblastoma pathway in liver tissue and hepatoma cells. Gastroenterology 2010;138:1920-30.

10. Logan JE, Mostofizadeh N, Desai AJ, VON Euw E, Conklin D, Konkankit V, et al. PD-0332991, a potent and selective inhibitor of cyclin-dependent kinase 4/6, demonstrates inhibition of proliferation in renal cell carcinoma at nanomolar concentrations and molecular markers predict for sensitivity. Anticancer Res 2013;33:2997-3004.
11. Puyol M, Martin A, Dubus P, Mulero F, Pizcueta P, Khan G, et al. A synthetic lethal interaction between K-Ras oncogenes and Cdk4 unveils a therapeutic strategy for non-small cell lung carcinoma. Cancer Cell 2010;18:63-73.
12. Rader J, Russell MR, Hart LS, Nakazawa MS, Belcastro LT, Martinez D, et al. Dual CDK4/CDK6 inhibition induces cell-cycle arrest and senescence in neuroblastoma. Clin Cancer Res 2013;19:6173-82.
13. Young RJ, Waldeck K, Martin C, Foo JH, Cameron DP, Kirby L, et al. Loss of CDKN2A expression is a frequent event in primary invasive melanoma and correlates with sensitivity to the CDK4/6 inhibitor PD0332991 in melanoma cell lines. Pigment Cell Melanoma Res 2014;27:590-600.
14. Nadji M, Gomez-Fernandez C, Ganjei-Azar P, Morales AR. Immunohistochemistry of estrogen and progesterone receptors reconsidered: experience with 5,993 breast cancers. Am J Clin Pathol 2005;123:21-27.
15. Sutherland RL, Green MD, Hall RE, Reddel RR, Taylor IW. Tamoxifen induces accumulation of MCF 7 human mammary carcinoma cells in the G0/G1 phase of the cell cycle. Eur J Cancer Clin Oncol 1983;19:615-21.
16. Finn RS, Dering J, Conklin D, Kalous O, Cohen DJ, Desai AJ, et al. PD 0332991, a selective cyclin D kinase 4/6 inhibitor, preferentially inhibits proliferation of luminal estrogen receptor-positive human breast cancer cell lines in vitro. Breast Cancer Res 2009;11:R77.
17. Trape AP, Liu S, Cortes AC, Ueno NT, Gonzalez-Angulo AM. Effects of CDK4/ 6 Inhibition in Hormone Receptor-Positive/Human Epidermal Growth Factor Receptor 2-Negative Breast Cancer Cells with Acquired Resistance to Paclitaxel. J Cancer 2016;7:947-56.
18. Anders L, Ke N, Hydbring P, Choi YJ, Widlund HR, Chick JM, et al. A systematic screen for CDK4/6 substrates links FOXM1 phosphorylation to senescence suppression in cancer cells. Cancer Cell 2011;20:620-34.
19. Hassanzadeh P. Colorectal cancer and NF-κB signaling pathway. Gastroenterol Hepatol Bed Bench 2011;4:127-32.
20. Wang W, Nag SA, Zhang R. Targeting the NF-κB signaling pathways for breast cancer Prevention and therapy. Curr Med Chem 2015; 22:264-89.
21. Whiteway SL, Harris PS, Venkataraman S, Alimova I, Birks DK, Donson AM, et al. Inhibition of cyclin-dependent kinase 6 suppresses cell proliferation and enhances radiation sensitivity in medulloblastoma cells. J Neurooncol. 2013;111:113-21.
22. Finn RS, Crown JP, Lang I, Boer K, Bondarenko IM, Kulyk SO, et al. The cyclin-dependent kinase 4/6 inhibitor palbociclib in combination with letrozole versus letrozole alone as first-line treatment of oestrogen receptor-positive, HER2-negative, advanced breast cancer (PALOMA-1/TRIO-18): a randomised phase 2 study. Lancet Oncol 2015;16:25-35.
23. Ehab M, Elbaz M. Profile of palbociclib in the treatment of metastatic breast cancer. Breast Cancer (Dove Med Press) 2016;8:83-91.
24. Turner NC, Ro J, André F, Loi S, Verma S, Iwata H, et al. Targeting the NF-κB signaling pathways for breast cancer Prevention and therapy. Curr Med Chem 2015;22:264-89
25. Fry DW, Harvey PJ, Keller PR, Elliott WL, Meade M, Trachet E, et al. Specific inhibition of cyclin-dependent kinase 4/6 by PD 0332991 and associated antitumor activity in human tumor xenografts. Mol Cancer Ther 2004;3:1427-38.
26. Rocca A, Farolfi A, Bravaccini S, Schirone A, Amadori D. Palbociclib (PD 0332991): targeting the cell cycle machinery in breast cancer. Expert Opin Pharmacother. 2014;15:407-20.
27. DeMichele A, Clark AS, Tan KS, Heitjan DF, Gramlich K, Gallagher M, et al. CDK 4/6 inhibitor palbociclib (PD0332991) in Rb+ advanced breast cancer: phase II activity, safety, and predictive biomarker assessment. Clin Cancer Res 2015;21:995-1001.
28. Finn RS, Martin M, Rugo HS, Jones S, Im SA, Gelmon K, et al. Palbociclib and Letrozole in Advanced Breast Cancer. N Engl J Med 2016;375:1925-36.
29. Flaherty KT, Lorusso PM, Demichele A, Abramson VG, Courtney R, Randolph SS, et al. Phase I, dose-escalation trial of the oral cyclin-dependent kinase 4/ 6 inhibitor PD 0332991, administered using a 21-day schedule in patients with advanced cancer. Clin Cancer Res 2012;18:568-76.
30. Schwartz GK, LoRusso PM, Dickson MA, Randolph SS, Shaik MN, Wilner KD, et al. Phase I study of PD 0332991, a cyclin-dependent kinase inhibitor, administered in 3-week cycles (Schedule 2/1). Br J Cancer 2011;104:1862-8.
31. Tamura K, Mukai H, Naito Y, Yonemori K, Kodaira M, Tanabe Y, et al. Phase I study of palbociclib, a cyclin-dependent kinase 4/6 inhibitor, in Japanese patients. Cancer Sci. 2016;107:755-63.

32. Hassanzadeh P, Atyabi F, Dinarvand R, Dehpour AR, Azhdarzadeh M, Dinarvand M. Application of nanostructured lipid carriers: the prolonged protective effects for sesamol in in vitro and in vivo models of ischemic stroke via activation of PI3K signalling pathway. Daru 2017;25:25.
33. Hassanzadeh P, Arbabi E, Rostami F, Atyabi F, Dinarvand R. Aerosol delivery of ferulic acid-loaded nanostructured lipid carriers: A promising treatment approach against the respiratory disorders. Physiol Pharmacol 2017;21:331-42.
34. Hassanzadeh P, Arbabi E, Atyabi F, Dinarvand R. Ferulic acid-loaded nanostructured lipid carriers: A promising nanoformulation against the ischemic neural injuries. Life Sci 2018;193:64-76.
35. Müller RH. Lipid nanoparticles: recent advances. Adv Drug Deliv Rev 2007;59:375-6.
36. Yang R, Zhang S, Kong D, Gao X, Zhao Y, Wang Z. Biodegradable polymer curcumin conjugate micelles enhance the loading and delivery of low potency curcumin. Pharm. Res 2012;29:3512-25.
37. Zhao J, Bai Y, Zhang C, Zhang X, Zhang YX, Chen J, et al., Cinepazide maleate protects PC12 cells against oxygen–glucose deprivation-induced injury. Neurol Sci 2014;35:875-81.
38. Russo J, Russo IH. Atlas and histologic classification of Tumors of rat mammary gland. J Mammary Gland Biol Neoplasia 2000;5:187-200.
39. Russo IH, Russo J. Mammary gland neoplasia in long-term rodent studies. Environ Health Prospect 1996;104:938-67.
40. Vijayaraghavan S, Karakas C, Doostan I, Chen X, Bui T, Yi M, et al. CDK4/6 and autophagy inhibitors synergistically induce senescence in Rb positive cytoplasmic cyclin E negative cancers. Nat Commun 2017;8:15916.
41. Ouyang Z, Wang S, Zeng M, Li Z, Zhang Q, Wang W, et al. Therapeutic effect of palbociclib in chondrosarcoma: implication of cyclin-dependent kinase 4 as a potential target. Cell Commun Signal 2019;17:17.
42. Bollard J, Miguela V, Ruiz de Galarreta M, Venkatesh A, Bian CB, Roberto MP, et al. Palbociclib (PD-0332991), a selective CDK4/6 inhibitor, restricts tumour growth in preclinical models of hepatocellular carcinoma. Gut 2017;66:1286-96.
43. Sacaan AI, Thibault S, Hong M, Kondegowda NG, Nichols T, Li R, et al. CDK4/6 Inhibition on Glucose and Pancreatic Beta Cell Homeostasis in Young and Aged Rats. Mol Cancer Res 2017;15 1531-41.
44. Hassanzadeh P, Ahmadiani A. Inflammatory pain induces neuronal alterations in NO and JNK dependent manners. DARU 2007;15:183-7.
45. Ahmadiani A. Hassanzadeh P, Aleboyeh M. Development of tolerance to anti-inflammatory effect of morphine. Arch Iranian Med 2003;6:307-9.
46. Ferrari M. Cancer nanotechnology: Opportunities and challenges. Nat Rev Cancer 2005;5:161-71.
47. Hassanzadeh P, Fullwood I, Sothi S, Aldulaimi D. Cancer nanotechnology. Gastroenterol Hepatol Bed Bench Spring 2011;4:63-9.
48. Hassanzadeh P, Atyabi F, Dinarvand R. Nanoparticles reshape the biomedical industry. Biomed Rev 2018;29:17-26.
49. Shi J, Kantoff PW, Wooster R, Farokhzad OC. Cancer nanomedicine: progress, challenges and opportunities. Nat Rev Cancer 2017;17:20-37.
50. Morawski AM, Winter PM, Crowder KC, Caruthers SD, Fuhrhop RW, Scott MJ, et al. Targeted nanoparticles for quantitative imaging of sparse molecular epitopes with MRI. Magn Reson Med 2004;51:480-6.
51. Cui Y, Qingqiao W, Hongkun P, Lieber CM. Nanowire nanosensors for highly sensitive and selective detection of biological and chemical species. Science 2011;293:1289-92.
52. Hassanzadeh P. New perspectives in biosensor technology. Gastroenterol Hepatol Bed Bench 2010;3:105-7.
53. Harishingani MG, Barentsz J, Hahn PF, Deserno WM, Tabatabaei S, van de Kaa CH, et al. Noninvasive detection of clinically occult lymph-node metastases in prostate cancer. N Engl J Med 2003;348:2491-9.
54. Park JW. Liposome-based drug delivery in breast cancer treatment. Breast Cancer Res 2002;4:95-9.
55. Kircher MF, Mahmood U, King RS, Weissleder R, Josephson L. A multimodal nanoparticle for preoperative magnetic resonance imaging and intraoperative optical brain tumor delineation. Cancer Res 2003;63:8122-5.
56. Li KC, Pandit SD, Guccione S, Bednarski MD. Molecular imaging applications in nanomedicine. Biomed Microdevices 2004;6:113-6.
57. Hirsch LR, Halas NJ, West JL. Nanoshell-mediated near-infrared thermal therapy of tumors under magnetic resonance guidance. Proc Natl Acad Sci USA 2003;100:13549-54.
58. Puri A, Loomis K, Smith B, Lee JH, Yavlovich A, Heldman E, et al. Lipid-based nanoparticles as pharmaceutical drug carriers: From concepts to clinic. Crit Rev Ther Drug Carrier Syst 2009;26:523-80.
59. Sai Li, Zhigui Su, Minjie Sun, Yanyu Xiao, Feng Cao, Aiwen Huang, et al. An arginine derivative contained nanostructure lipid carriers with pH-sensitive membranolytic capability for lysosomolytic anticancer

drug delivery. Int J Pharm 2012;436:248-57.

60. Shenoy VS, Vijay IK, Murthy RS. Tumour targeting: biological factors and formulation advances in injectable lipid nanoparticles. J Pharm Pharmacol 2005;57:411-21.
61. Bondì ML, Azzolina A, Craparo EF, Botto C, Amore E, Giammona G, et al. Entrapment of an EGFR inhibitor into nanostructured lipid carriers (NLC) improves its antitumor activity against human hepatocarcinoma cells. J Nanobiotechnol 2014;12:21.
62. Barrett JC. Mechanisms of multistep carcinogenesis and carcinogen risk assessment. Environ Health Perspect 1993;100:9-20.
63. Manna S, Chakraborty T, Damodaran S, Samanta K, Rana B, Chatterjee M. Protective role of fish oil (Maxepa) on early events of rat mammary carcinogenesis by modulation of DNA-protein crosslinks, cell proliferation and p53 expression. Cancer Cell Int 2007;7:6.